

Fermi National Accelerator Laboratory

FERMILAB-PUB-91/284-T

ANL-HEP-PR-91-94

DTP/91/70

October 1991

Transverse Momentum Distribution of Z -Boson Pairs at Hadron Supercolliders

T. Han,¹ R. Meng,² J. Ohnemus^{1,2,3}

¹*Fermi National Accelerator Laboratory, P. O. Box 500, Batavia, IL 60510, USA*

²*High Energy Physics Division, Argonne National Laboratory, Argonne, IL 60439, USA*

³*Department of Physics, University of Durham, Durham, DH1 3LE, England*

ABSTRACT

We present the transverse momentum distribution of the Z -pairs for $pp \rightarrow ZZX$ at supercollider energies. The full $p_T(ZZ)$ spectrum is obtained by matching the low- p_T result (from soft gluon resummation to all orders in α_s) to the high- p_T result (from the $\mathcal{O}(\alpha_s)$ perturbative calculation). We examine where the fixed $\mathcal{O}(\alpha_s)$ perturbative calculation is unreliable. We also present a comparison of our result with the Monte Carlo program PYTHIA. The results are significant for background calculations to heavy Higgs boson searches at hadron supercolliders, as well as for testing perturbative QCD.



I. INTRODUCTION

The Standard Model (SM) has been amazingly successful in describing the strong and electroweak interactions in high energy physics. However, the electroweak symmetry breaking mechanism remains a mystery and the experimental search for the neutral Higgs boson (H) predicted by the SM is still a major challenge[1]. If the mass of the Higgs boson (m_H) is heavier than the mass of the Z -boson (M_Z), then the next generation of hadron supercolliders will be the appropriate tools for discovering the Higgs boson. Due to the enhanced couplings of a heavy Higgs boson to vector boson pairs and the distinctive experimental signature, the decay mode $H \rightarrow ZZ$ or $ZZ^* \rightarrow \ell^+\ell^-, \ell^+\ell^-$ ($\ell = e, \mu$) is considered the most promising channel for discovering the Higgs boson if $140 \text{ GeV} < m_H < 800 \text{ GeV}$ [1]. The principal production mechanisms for this channel at hadron colliders are the gluon fusion process $gg \rightarrow H \rightarrow ZZ$ [2] and the electroweak boson fusion process $qq \rightarrow qqVV \rightarrow qqH \rightarrow qqZZ$ ($V = W, Z$)[3, 4]. For a top quark mass of 150 GeV the gluon fusion process is dominant for Higgs boson masses up to $m_H \approx 800 \text{ GeV}$, while the importance of the electroweak boson fusion process increases as the Higgs boson mass becomes larger and is comparable to the gluon fusion process when $m_H \gtrsim 800 \text{ GeV}$.

The major background to the heavy Higgs boson signal is continuum ZZ production from the subprocess

$$q\bar{q} \rightarrow ZZ \tag{1}$$

which was first calculated in Ref. [5]. The production of Z -pairs in association with one or two QCD jets has also been calculated[6, 7]. Recently the complete $\mathcal{O}(\alpha_s)$ QCD corrections to hadronic ZZ production have also been calculated[8, 9]. The $\mathcal{O}(\alpha_s)$ calculation includes the virtual gluon correction to Eq. (1) and the real emission subprocesses

$$q\bar{q} \rightarrow ZZg, \quad qg \rightarrow ZZq, \quad \bar{q}g \rightarrow ZZ\bar{q}. \tag{2}$$

If the mass of the Higgs boson is as heavy as 800 GeV, the width of the Higgs boson is

so broad that a clear resonance structure is lost. In this case it is important to understand and suppress the backgrounds as much as possible in order to definitively identify the heavy Higgs boson. Tagging the spectator jets in the electroweak boson fusion process has been suggested as a way to suppress the continuum ZZ background[10]. A recent study showed that tagging a *single* low transverse momentum (p_T) jet in the forward-backward region may be a very effective way to enhance the signal-to-background ratio for the heavy Higgs boson[4]. Although it may not be necessary to study the jet activities for a Higgs boson if $2M_Z < m_H \leq 600$ GeV due to the rather clear resonance in the M_{ZZ} distribution[11], single jet-tagging would still be useful for singling out the electroweak boson fusion process in order to study the HWW and HZZ couplings[4]. In the strongly interacting scenario of the electroweak symmetry breaking[12], single jet-tagging would also be helpful to select events from the longitudinally polarized vector boson scatterings[4].

The Z -pair from the decay of the Higgs boson populate the relatively low- p_T region, *i.e.*, $p_T(ZZ)$ is of order M_W for the electroweak boson fusion process and of order 20-40 GeV for the gluon fusion process after soft gluon resummation[13]. The fixed order perturbative QCD background calculations in Refs. [6–8], which have served as the basis for many background studies, can predict the $p_T(ZZ)$ behavior in the high transverse momentum region, but fail to describe the spectrum in the relatively low- $p_T(ZZ)$ region. It is therefore imperative to carry out a more reliable calculation for continuum ZZ production in the low- p_T region and see quantitatively to what extent the $\mathcal{O}(\alpha_s)$ perturbative result is valid in this kinematical regime.

In this paper, we calculate the $p_T(ZZ)$ spectrum for the process

$$p + p \rightarrow Z + Z + X . \tag{3}$$

In the low- $p_T(ZZ)$ region, we carry out a resummation of soft gluon emission to all orders in α_s [13–19]. In the high- $p_T(ZZ)$ region, we use the fixed $\mathcal{O}(\alpha_s)$ perturbative calculation

for the spectrum. The low- p_T result is then matched to the high- p_T result to obtain the full $p_T(ZZ)$ spectrum. We find that the $p_T(ZZ)$ spectrum from the $\mathcal{O}(\alpha_s)$ calculation is unreliable for $p_T(ZZ) < 25$ (35) GeV at the LHC (SSC) energy. If one is interested in the kinematical region of the ZZ invariant mass $M_{ZZ} > 500$ GeV, which may be relevant to heavy Higgs boson searches, one has to require $p_T(ZZ) > 30$ (45) GeV at the LHC (SSC) energy in order to assure the validity of the $\mathcal{O}(\alpha_s)$ perturbative calculation. To see how well a typical shower Monte Carlo program predicts the $p_T(ZZ)$ spectrum, we also present a comparison with the Monte Carlo result from PYTHIA[20]. The results agree reasonably well in the low- $p_T(ZZ)$ region, but PYTHIA significantly underestimates the spectrum in the high- $p_T(ZZ)$ region.

The remainder of this paper is organized as follows. In Sec. II we present the formalism for calculating the $p_T(ZZ)$ distribution for hadronic Z -pair production and we describe how to match the resummed result in the low- p_T region to the $\mathcal{O}(\alpha_s)$ result in the high- p_T region. Results and discussions for the $p_T(ZZ)$ distribution at hadron supercolliders are given in Sec. III. Summary and conclusions are given in Sec. IV. Details on extracting the resummation coefficients are presented in an Appendix.

II. FORMALISM FOR $P_T(ZZ)$ DISTRIBUTION

The formalism for calculating the $p_T(ZZ)$ distribution for hadronic Z -pair production is presented in this section. We first describe the soft gluon resummation techniques used to calculate the low- $p_T(ZZ)$ spectrum. Later we discuss how to match the resummed result in low- p_T region to the $\mathcal{O}(\alpha_s)$ perturbative result in the high- p_T region.

A. Low- $p_T(ZZ)$ Distribution from Soft Gluon Resummation

In perturbative QCD at large and moderate values of $p_T(ZZ)$, $p_T(ZZ) \gtrsim \mathcal{O}(M_{ZZ})$, the cross section for hadronic Z -pair production can be computed by truncating the α_s power

series expansion

$$\frac{d^2\sigma}{dQ^2 dp_T^2} = \alpha^2 \alpha_s (a_1 + a_2 \alpha_s + a_3 \alpha_s^2 + \dots), \quad (4)$$

however, at low p_T , $p_T \ll \mathcal{O}(Q)$, the convergence of the perturbative series deteriorates. Here and henceforth, p_T denotes the transverse momentum of the Z -pair, Q is the invariant mass of the Z -pair, M_{ZZ} , and α and α_s denote the electromagnetic and strong couplings, respectively. In the limit $p_T/Q \rightarrow 0$, the dominant contributions (*i.e.*, the leading logarithmic contributions) to Eq. (4) have the form

$$\frac{d^2\sigma}{dQ^2 dp_T^2} \sim \frac{\alpha^2 \alpha_s}{p_T^2} \ln\left(\frac{Q^2}{p_T^2}\right) \left[b_1 + b_2 \alpha_s \ln^2\left(\frac{Q^2}{p_T^2}\right) + b_3 \alpha_s^2 \ln^4\left(\frac{Q^2}{p_T^2}\right) + \dots \right]. \quad (5)$$

The convergence of the series is therefore governed by $\alpha_s \ln^2(Q^2/p_T^2)$ instead of α_s . The double-logarithms come from soft and collinear gluon emissions. At sufficiently low p_T , $\alpha_s \ln^2(Q^2/p_T^2)$ will be large even when α_s is small. Thus, it would be meaningless to calculate the low- p_T spectrum by truncating the power series at any given order of α_s . One is forced to include all the large logarithmic contributions to all orders in α_s when calculating the p_T spectrum in this kinematic region. Fortunately, the coefficients b_i of the leading-logarithm approximation in Eq. (5) are not independent and it is possible to sum the series exactly[14] so that it may be applied even when $\alpha_s \ln^2(Q^2/p_T^2)$ is large. This technique has been generalized by Collins and Soper[15] to resum all terms in the perturbation series that are at least as singular as $1/p_T^2$ when $p_T \rightarrow 0$ and their formalism has been applied to Drell-Yan lepton-pair production[16], single vector boson production[17, 18], Higgs boson production[13], and heavy quark-pair production[19]. Following the same procedure, the resummed formula for hadronic Z -pair production can be written as

$$\frac{d^3\sigma}{dQ^2 dp_T^2 dy} (\text{resum}) = \sum_{q=u,d,s,\dots} \hat{\sigma}_{q\bar{q}}^{(0)}(Q^2) \frac{1}{S} \int \frac{d^2\vec{b}}{4\pi} e^{i\vec{b}\cdot\vec{p}_T} W(b), \quad (6)$$

where

$$\begin{aligned}
W(b) = \exp \left\{ - \int_{C_1^2/b^2}^{C_2^2 Q^2} \frac{dq^2}{q^2} \left[\ln \left(\frac{C_2^2 Q^2}{q^2} \right) A(\alpha_s(q^2)) + B(\alpha_s(q^2)) \right] \right\} \\
\times \left\{ \left(C \otimes f_{q/p} \right) \left(x_a, \frac{C_3^2}{b^2} \right) \left(C \otimes f_{\bar{q}/p} \right) \left(x_b, \frac{C_3^2}{b^2} \right) + (x_a \leftrightarrow x_b) \right\}.
\end{aligned} \tag{7}$$

The factor $W(b)$ is a Sudakov-like form factor, y is the rapidity of the Z -pair, S is the square of the hadronic center of mass energy, and $\hat{\sigma}_{q\bar{q}}^{(0)}(Q^2)$ is the lowest order parton-level cross section for $q\bar{q} \rightarrow ZZ$ production,

$$\hat{\sigma}_{q\bar{q}}^{(0)}(Q^2) = \frac{\pi\alpha^2}{3Q^2} \left[(g_-^{qZq})^4 + (g_+^{qZq})^4 \right] \left[\left\{ \frac{4 + (1 - \beta^2)^2}{1 + \beta^2} \right\} \ln \left(\frac{1 + \beta}{1 - \beta} \right) - 2\beta \right], \tag{8}$$

with $\beta = \sqrt{1 - 4M_Z^2/Q^2}$. The right- and left-handed Z -boson-to-quark couplings are denoted by g_{\pm}^{qZq} :

$$\begin{aligned}
g_+^{qZq} &= -Q_q \tan \theta_w, \\
g_-^{qZq} &= \frac{T_3^q}{\sin \theta_w \cos \theta_w} - Q_q \tan \theta_w,
\end{aligned} \tag{9}$$

where Q_q and T_3^q denote the electric charge (in units of the proton charge e) and the third component of weak isospin of the quark q , and θ_w is the Weinberg weak mixing angle. The parton momentum fractions in the limit $p_T/Q \rightarrow 0$ are

$$x_a = e^y \sqrt{\frac{Q^2}{S}}, \quad x_b = e^{-y} \sqrt{\frac{Q^2}{S}}. \tag{10}$$

and $f_{q/p}(x_a)$, $f_{\bar{q}/p}(x_b)$ are the quark and anti-quark distribution functions inside the protons. The integration variable b is the impact parameter (conjugate variable to p_T). The parameters C_1 , C_2 , and C_3 are unphysical and arbitrary, corresponding to renormalization and factorization scale choices. Following previous authors, our canonical choices for these parameters are

$$C_1 = C_3 = 2e^{-\gamma_B} \equiv b_0, \quad C_2 = 1, \tag{11}$$

where γ_E is Euler's constant. The symbol \otimes denotes a convolution defined by

$$(f \otimes g)(x) \equiv \int_x^1 f(y) g\left(\frac{x}{y}\right) \frac{dy}{y}. \quad (12)$$

The functions A , B , and $C(x)$ have perturbative expansions in α_s :

$$\begin{aligned} A(\alpha_s) &= \sum_{n=1}^{\infty} A^{(n)} \left(\frac{\alpha_s}{2\pi}\right)^n, \\ B(\alpha_s) &= \sum_{n=1}^{\infty} B^{(n)} \left(\frac{\alpha_s}{2\pi}\right)^n, \\ C(x, \alpha_s) &= \delta(1-x) + \sum_{n=1}^{\infty} C^{(n)}(x) \left(\frac{\alpha_s}{2\pi}\right)^n. \end{aligned} \quad (13)$$

Therefore once the power series expansion coefficients for A , B , and C are known, the p_T distribution in the low- p_T region can be calculated using Eqs. (6) and (7).

The coefficients $A^{(n)}$, $B^{(n)}$, and $C^{(n-1)}$ can be obtained by formally expanding Eq. (6) in terms of α_s to the first n terms and then comparing with the fixed n^{th} order perturbative calculation in the asymptotic limit of small p_T . In this paper, we are working in perturbation theory to first order in α_s for large p_T , thus we will truncate the series with $A^{(1)}$, $B^{(1)}$, and $C^{(0)} = \delta(1-x)$. Neglecting $C^{(1)}$ will only affect the normalization at $p_T = 0$ to $\mathcal{O}(\alpha_s)$ and the distribution for $p_T \neq 0$ to $\mathcal{O}(\alpha_s^2)$. This implies that our calculation includes the resummation of next-to-leading logarithms to all orders in α_s , but the total integrated cross section is accurate to zeroth order in α_s .

To extract the coefficients $A^{(1)}$ and $B^{(1)}$, one formally expands the resummed result of Eq. (6) to first order in $\alpha_s(\mu)$ and gets the asymptotic result for low p_T at a fixed renormalization scale μ . The parton distribution functions are evaluated at a fixed factorization scale M . The resulting asymptotic expression is

$$\begin{aligned}
\frac{d^3\sigma}{dQ^2 dp_T^2 dy} \text{ (asym)} = & \\
& \sum_{q=u,d,s,\dots} \hat{\sigma}_{q\bar{q}}^{(0)}(Q^2) \frac{1}{S} \frac{\alpha_s}{2\pi} \frac{1}{p_T^2} \left\{ \left[A^{(1)} \ln\left(\frac{Q^2}{p_T^2}\right) + B^{(1)} \right] \left[f_{q/p}(x_a) f_{\bar{q}/p}(x_b) + (x_a \leftrightarrow x_b) \right] \right. \\
& + \left[f_{q/p}(x_a) \left(P_{\bar{q}\bar{q}} \otimes f_{\bar{q}/p} \right)(x_b) + f_{\bar{q}/p}(x_a) \left(P_{qq} \otimes f_{q/p} \right)(x_b) + (x_a \leftrightarrow x_b) \right] \\
& \left. + \left[f_{q/p}(x_a) \left(P_{\bar{q}g} \otimes f_{g/p} \right)(x_b) + f_{\bar{q}/p}(x_a) \left(P_{qg} \otimes f_{g/p} \right)(x_b) + (x_a \leftrightarrow x_b) \right] \right\}. \tag{14}
\end{aligned}$$

The parton splitting functions are

$$\begin{aligned}
P_{qg}(x) &= \frac{1}{2} \left(x^2 + (1-x)^2 \right), \\
P_{qq}(x) &= \frac{4}{3} \left(\frac{1+x^2}{1-x} \right)_+, \tag{15}
\end{aligned}$$

where the “+” distribution is defined by

$$\int_0^1 dx f_+(x) h(x) \equiv \int_0^1 dx f(x) (h(x) - h(1)). \tag{16}$$

Starting with the $\mathcal{O}(\alpha_s)$ perturbative calculation of hadronic Z -pair production in Ref. [8], taking the limit of $p_T \rightarrow 0$, and comparing with the asymptotic expression in Eq. (14), we find

$$A^{(1)} = 2 C_F, \quad B^{(1)} = -3 C_F, \tag{17}$$

where $C_F = 4/3$ is the color factor for the quark-gluon vertex. These coefficients are identical to those in the Drell-Yan process[16–18] since the physics of the initial state soft and collinear gluon emissions are the same in the two cases although the Feynman diagrams and the kinematics in the ZZ case are much more complicated. Details on the derivation of $A^{(1)}$ and $B^{(1)}$ are given in the Appendix.

The b -space Fourier transform in Eq. (6) can be simplified by using the identity

$$\int \frac{d^2\vec{b}}{(2\pi)^2} e^{i\vec{b}\cdot\vec{p}_T} W(b) = \int_0^\infty \frac{b db}{2\pi} J_0(b p_T) W(b), \quad (18)$$

where $J_0(x)$ is the zeroth order Bessel function. Using this identity and the parameters given in Eq. (11), the resummed formula in Eq. (6) for low p_T hadronic Z -pair production can be rewritten as

$$\frac{d^3\sigma}{dQ^2 dp_T^2 dy} (\text{resum}) = \sum_{q=u,d,s,\dots} \hat{\sigma}_{q\bar{q}}^{(0)}(Q^2) \frac{1}{2S} \int_0^\infty b db J_0(b p_T) W(b), \quad (19)$$

where

$$W(b) = \exp \left\{ - \int_{b_0^2/b^2}^{Q^2} \frac{dq^2}{q^2} \frac{\alpha_s(q^2)}{2\pi} C_F \left[2 \ln \left(\frac{Q^2}{q^2} \right) - 3 \right] \right\} \\ \times \left\{ f_{q/p} \left(x_a, \frac{b_0^2}{b^2} \right) f_{\bar{q}/p} \left(x_b, \frac{b_0^2}{b^2} \right) + (x_a \leftrightarrow x_b) \right\}. \quad (20)$$

B. Full p_T (ZZ) Spectrum

Having obtained the formula for the low- p_T distribution, we now discuss the calculation of the high- p_T distribution. At high p_T , the p_T spectrum can be reliably calculated from conventional $\mathcal{O}(\alpha_s)$ perturbation theory[6–8]. The cross section is

$$d\sigma(pp \rightarrow ZZX) (\text{pert}) = \sum_{i,j=q,\bar{q},g} \int dx_a dx_b f_{i/p}(x_a, M^2) f_{j/p}(x_b, M^2) d\hat{\sigma}^{(1)}(ij \rightarrow ZZX), \quad (21)$$

where $d\hat{\sigma}^{(1)}$ is the partonic cross section obtained by calculating the Feynman diagrams at $\mathcal{O}(\alpha_s)$ in perturbation theory, $f_{i/p}$ are the parton distribution functions, and the sum is over all possible partons contributing to the three subprocesses $q\bar{q} \rightarrow ZZg$, $qg \rightarrow ZZq$, and $\bar{q}g \rightarrow ZZ\bar{q}$. The squared matrix elements for these subprocesses are given in Ref. [8]. It is straightforward to calculate $d^2\sigma/dQ^2 dp_T^2$ or $d\sigma/dp_T^2$ via numerical Monte Carlo integration methods.

We now have formulas for the low- p_T region from the soft gluon resummation and for the high- p_T region from the $\mathcal{O}(\alpha_s)$ perturbative calculation. In the low- p_T region, the resummed

result is an accurate representation of the p_T spectrum. As p_T gets large, however, the non-leading terms, *i.e.*, those terms which are less singular than $1/p_T^2$ and were not resummed, become important and need to be included. These non-leading terms can be estimated to first order in α_s by using the difference between the perturbative and the asymptotic formulas and the following matching treatment was proposed[17, 18] for the p_T spectrum

$$\frac{d^2\sigma}{dQ^2 dp_T^2}(\text{resum}) + \left[\frac{d^2\sigma}{dQ^2 dp_T^2}(\text{pert}) - \frac{d^2\sigma}{dQ^2 dp_T^2}(\text{asym}) \right]. \quad (22)$$

Notice that the perturbative and the asymptotic contributions cancel each other in the limit $p_T \rightarrow 0$ to give the resummed result. This matched result extends to a quite large- p_T region, but as p_T gets even larger, eventually the basic argument for large-log resummation becomes invalid and the fixed $\mathcal{O}(\alpha_s)$ result represents the more accurate p_T spectrum. Thus in principle, one should switch from the matched result to the perturbative result around some value p_T^{match} by some procedure. Also notice that the resummed and the asymptotic results cancel each other to first order in α_s , so the perturbative term in Eq. (22) should dominate at large- p_T , as one would hope. Unfortunately, although it is formally of $\mathcal{O}(\alpha_s^2)$, the difference between the resummed and the asymptotic results may be much larger than the perturbative result in the large- p_T limit. This is because the resummed and asymptotic calculations are valid only in the low- p_T region and they do not exhibit the correct high- p_T behavior, especially after convolution with the parton distribution functions which were evaluated at the x values given by Eq. (10) corresponding to $p_T = 0$. This also makes the switching necessary in practice.

The boundary line, p_T^{match} , above which the perturbative result is more accurate than the matched result can be estimated by the condition

$$\alpha_s(p_T^2) \ln^2 \frac{Q^2}{p_T^2} \approx \mathcal{O}(1) \quad (23)$$

which follows from Eq. (5). To a good approximation, we find that $p_T^{\text{match}} \approx Q/3$. However, there does not exist a well prescribed procedure derived from first principle for the switching;

the procedure has to be chosen by trial and error according to the numerical outcome. In practice, a function

$$f(p_T) = \frac{1}{1 + (p_T/p_T^{\text{match}})^4}, \quad (24)$$

has been introduced by Kauffman[13] to smoothly switch from the matched formula to the perturbative formula according to

$$\frac{d^2\sigma}{dQ^2 dp_T^2}(\text{full}) = \frac{d^2\sigma}{dQ^2 dp_T^2}(\text{pert}) + f(p_T) \left[\frac{d^2\sigma}{dQ^2 dp_T^2}(\text{resum}) - \frac{d^2\sigma}{dQ^2 dp_T^2}(\text{asym}) \right]. \quad (25)$$

The functional form of $f(p_T)$ was chosen to minimize the error introduced by the switching. As $p_T \rightarrow 0$, the high power $(p_T/p_T^{\text{match}})^4$ insures that $f(p_T) \rightarrow 1$ quickly so that the matched result is obtained. As $p_T \rightarrow \infty$, the high power $(p_T/p_T^{\text{match}})^4$ also insures that $f(p_T) \rightarrow 0$ quickly so that the perturbative result is recovered. The error introduced by the matching procedure is of $\mathcal{O}(\alpha_s^2)$ [13, 18]. Equation (25) will serve as our formula for the full p_T distribution.

Before carrying out numerical calculations, some remarks are in order. It has been pointed out by Parisi and Petronzio[14] that the resummed expression Eq. (19) is ill-defined when $b \geq 1/\Lambda_{QCD}$ because confinement sets in and α_s diverges. Several procedures have been proposed in the literature[15–17] to cut-off the divergence and parameterize the non-perturbative effects. In this paper we follow the procedure used by Collins *et al.*[15] and Davies *et al.*[16]; we replace $W(b)$ in Eq. (20) by

$$W(b) \rightarrow W(b_*) e^{-S_{np}(b)} \quad (26)$$

where

$$b_* = \frac{b}{\sqrt{1 + b^2/b_{max}^2}} \quad (27)$$

cuts off large values of b at some b_{max} and $S_{np}(b)$ parameterizes the large- b dependence controlled by nonperturbative physics. In principle $\exp[-S_{np}(b)]$ can be measured, but in practice one can approximate it with a simple Gaussian parameterization,

$$S_{np}(b) = b^2 \left[g_1 + g_2 \ln \left(\frac{b_{max} Q}{2} \right) \right], \quad (28)$$

where according to Davies *et al.*[16]

$$g_1 = 0.15 \text{ GeV}^2, \quad g_2 = 0.4 \text{ GeV}^2, \quad b_{max} = (2 \text{ GeV})^{-1}. \quad (29)$$

The g_1 and g_2 are obtained by fitting Drell-Yan data. We will take these values as our standard choice and will study the uncertainty arising from different choices in the next section.

Some care needs to be taken when numerically evaluating the resummed result in Eq. (19). For a very low- p_T value, integrating over a few periods of the Bessel function $J_0(b p_T)$ will cover a large b -range. In this case the exponentially damping factor $\exp(-S_{np})$ sets in quickly and the integral converges rapidly. However, for large p_T , many periods of the Bessel function may still be in the small b -region and one must integrate over many more periods in order to get a reliable result. To improve the efficiency of our numerical programs, we employ the methods of Ref. [18], namely, we numerically integrate Eq. (19) over the first 15 or so periods of the Bessel function and then use an asymptotic expansion for the Fourier transform[21].

III. $P_T(ZZ)$ DISTRIBUTION AT HADRON SUPERCOLLIDERS

In this section we calculate the $p_T(ZZ)$ distributions at the supercollider energies, namely, 15.4 TeV for the LHC and 40 TeV for the SSC. We also compare our results with results from the shower Monte Carlo program PYTHIA and we discuss the theoretical uncertainties in our calculations.

The numerical work for this paper was done using the one-loop expression for α_s with $N_f = 5$. The QCD scale Λ_5 is obtained by evolving $\alpha_s(q^2)$ from $N_f = 4$ to $N_f = 5$ such that $\alpha_s(q^2)$ is a continuous function of q^2 ; the b -quark mass is taken to be $m_b = 5 \text{ GeV}$ and the four-flavor QCD scale Λ_4 is determined by the choice of parton distribution functions.

We work in the $\overline{\text{MS}}$ scheme[22] for renormalization and factorization and set the two scales to be equal $\mu = M = Q$, where Q is the invariant mass of the Z -pair. For most of our numerical presentations, we use the parton distribution functions from Harriman, Martin, Roberts, and Stirling (HMRS Set B)[23], we will however, compare these results with results from Morfin and Tung distribution functions (Set B1)[24].

Figure 1 shows the calculated differential distributions $d^2\sigma/dQ dp_T$ at the LHC for $Q = 200, 500, \text{ and } 800$ GeV versus p_T . The four curves shown are the perturbative, asymptotic, resummed, and full matched results. The full matched curve represents the resummed result in the region $p_T < p_T^{\text{match}} = Q/3$ and smoothly transforms to the perturbative result at higher p_T . At very low p_T , the perturbative result diverges and becomes significantly different from the resummed result below $p_T = 25, 30, \text{ and } 40$ GeV for $Q = 200, 500, \text{ and } 800$ GeV, respectively. Figure 2 is the same as Fig. 1 except it is for the SSC energy. In Fig. 2 the perturbative result diverges from the resummed curve below $p_T = 35, 45, \text{ and } 60$ GeV for $Q = 200, 500, \text{ and } 800$ GeV. The Q -dependence of the minimal- p_T value below which the perturbative calculation is invalid is a reflection of the large-log terms $\ln^2(Q^2/p_T^2)$. From this observation, based on our numerical results, we approximate an empirical linear relation between Q and p_T^{cut} below which the perturbative result will not be reliable,

$$p_T^{\text{cut}} = \frac{1}{k} Q + p_T^0, \quad (30)$$

where

$$k = 40, \quad p_T^0 = 20 \text{ GeV}, \quad \text{for the LHC}, \quad (31)$$

and

$$k = 24, \quad p_T^0 = 26 \text{ GeV}, \quad \text{for the SSC}. \quad (32)$$

This empirical relationship between p_T^{cut} and Q gives a rough estimate of the kinematical

region where the $\mathcal{O}(\alpha_s)$ perturbative calculation of Z -pair production is invalid and it also can be implemented into the Monte Carlo perturbative calculation as a cut.

Figure 3 gives the p_T distributions integrated over Q for the LHC and SSC in parts a) and b), respectively. The resummed, perturbative, and full matched results are shown in the figure. To assure that the Z -pairs are produced in the central region within the detector coverage, in Fig. 3 we have imposed a cut on the Z -pair rapidity

$$|y(ZZ)| < 2 \quad \text{and} \quad M_{ZZ} < 2 \text{ TeV.} \quad (33)$$

Also shown in Fig. 3 is the p_T distribution generated by the shower Monte Carlo program PYTHIA[20]. Shower Monte Carlo programs use the Sudakov form factor as a weight to generate the soft gluon radiations based on a hard scattering matrix element. These programs have been widely used in experimental simulations. In the low- p_T region, the results agree reasonably well, however, at $p_T > 100$ GeV, the PYTHIA result falls off sharply and significantly underestimates the high- p_T spectrum. The discrepancy at high p_T occurs because PYTHIA starts generating soft gluon radiation from the lowest order $q\bar{q} \rightarrow ZZ$ matrix element which has $p_T(ZZ) = 0$. Thus it is very inefficient at producing gluons in the high- p_T region. On the other hand, our result for the high- p_T region is based on the $2 \rightarrow 3$ matrix elements of Ref. [8].

We now discuss the theoretical uncertainties in our calculations. First of all, the error introduced by the matching procedure in the intermediate- p_T region is of $\mathcal{O}(\alpha_s^2)$ [13,18], which is at the few percent level. Secondly, higher order contributions from $C^{(1)}$, $A^{(2)}$, $B^{(2)}$, *etc.* in Eq. (13) have been ignored. Neglecting those may introduce an error of about 30%[8,25].

Another source of uncertainties at low p_T is from the non-perturbative treatment, namely, the parameters g_1 , g_2 , and b_{max} in Eq. (28). The parameter b_{max} is a value above which perturbative QCD breaks down. Davies *et al.*[16] took $b_{max} = (2 \text{ GeV})^{-1}$, which is near the lowest value allowed for the factorization scale in the parton distribution functions.

The parameters g_1 and g_2 are then determined by fitting Drell-Yan data at $\sqrt{S} = 27$ and 62 GeV. To study the sensitivity of our results to these parameters, we fix b_{max} and change the standard choice of g_1 and g_2 in Eq. (29) by factors of 2 and 1/2, which gives

$$g_1 = 0.300 \text{ GeV}^2, \quad g_2 = 0.8 \text{ GeV}^2, \quad (34)$$

and

$$g_1 = 0.075 \text{ GeV}^2, \quad g_2 = 0.2 \text{ GeV}^2. \quad (35)$$

Figure 4 compares the resummed results for the differential distribution $d^2\sigma/dQ dp_T$ at the SSC for $Q = 200$ GeV using these parameters. We find that at $p_T \simeq 2$ GeV, the deviation from the result of the standard choice is about 15%, while at the peak region $p_T \simeq 10$ GeV, the deviation drops to about 2%. Since we are interested in the relatively large- p_T region, the uncertainty from the non-perturbative parameterization does not affect our previous discussion.

Next we examine the uncertainty from the choice of parton distribution functions. Figure 5 compares the $d^2\sigma/dQ dp_T$ distribution at the SSC for $Q = 200$ and 800 GeV for the HMRS Set B and MT Set B1 parton distribution functions. We see that the result from MT is higher than that of HMRS by about 20% near the peak value for $Q = 200$ GeV, while they tend to agree better at larger p_T . The difference between HMRS and MT also becomes much smaller for $Q = 800$ GeV. This uncertainty is mainly due to our ignorance of the parton distributions in the small x region.

IV. CONCLUSIONS

We have calculated the transverse momentum distribution for hadronic Z -pair production at hadron supercolliders. The full $p_T(ZZ)$ spectrum is obtained by matching the resummed result at low $p_T(ZZ)$ to the perturbative result at high $p_T(ZZ)$. We find that the perturbative $\mathcal{O}(\alpha_s)$ calculation is invalid for $p_T(ZZ) < 25$ (35) GeV at the LHC (SSC)

energy. In heavy Higgs boson searches, a minimum cutoff on M_{ZZ} may be needed in order to suppress the ZZ + jet backgrounds. However, in order to make the $\mathcal{O}(\alpha_s)$ background calculation reliable, an increasing cutoff on p_T is also necessary. We have shown that to avoid large logarithms of the form $\ln(p_T^2/M_{ZZ}^2)$ that spoil the $\mathcal{O}(\alpha_s)$ perturbative calculation, we need to impose, *e.g.*, $p_T(ZZ) > 45$ GeV for $M_{ZZ} > 500$ GeV, and $p_T(ZZ) > 60$ GeV for $M_{ZZ} > 800$ GeV at the SSC energy.

We have also compared our results for the $p_T(ZZ)$ distribution with shower Monte Carlo results from PYTHIA. We find that they agree reasonably well in shape for $p_T(ZZ) < 100$ GeV, however, PYTHIA significantly underestimates the rate for large $p_T(ZZ)$. The discrepancy at large $p_T(ZZ)$ is easily understood since PYTHIA starts generating the ZZ events from the $q\bar{q} \rightarrow ZZ$ matrix element with zero $p_T(ZZ)$.

Our results are not sensitive to the non-perturbative parameterization since we are mainly interested in rather large p_T , where the perturbative contribution is dominant. Different choices of the parton distribution functions give about 20% uncertainty at the peak p_T region while the difference tends to be smaller at larger p_T values.

Since the $p_T(ZZ)$ spectrum is entirely governed by QCD radiations and the ZZ production rate at supercollider energies is sizable, our results could also provide a good test of perturbative QCD at a scale of order 200 GeV.

ACKNOWLEDGMENTS

The authors would like to thank P. Arnold, R. K. Ellis, R. Kauffman, and J. F. Owens for useful discussions. J. O. would also like to thank the Fermilab theory group and the Argonne National Laboratory HEP theory group for hospitality and support during the initial stages of this work. This research was supported in part by the U. S. Department of Energy under contract number DE-FG05-87-ER40319 and W-31-109-ENG-38.

APPENDIX: EXTRACTION OF RESUMMATION COEFFICIENTS

In this appendix we discuss the derivation of the coefficients $A^{(1)}$ and $B^{(1)}$ in Eq. (17). We begin by examining the asymptotic expression in Eq. (14) which can be viewed as a convolution of the parton distribution functions with the asymptotic partonic differential cross section, $d^3\hat{\sigma}_{ij}^{\text{asym}}/dQ^2 dp_T^2 dy$, summed over the $2 \rightarrow 3$ real emission subprocesses $q\bar{q} \rightarrow ZZg$, $qg \rightarrow ZZq$, and $g\bar{q} \rightarrow ZZ\bar{q}$. We first observe that the terms proportional to the Altarelli-Parisi splitting functions are proportional to $1/p_T^2$ and are divergent as $p_T \rightarrow 0$. These terms are mass singular terms and will give pure $1/\epsilon$ collinear poles in the dimensional regularization scheme[26]. These poles must be factorized into the $\overline{\text{MS}}$ [22] definition of the parton distribution functions. Putting the Altarelli-Parisi splitting terms aside, deconvoluting Eq. (14), and using the variable transformation $dQ^2 dy = S dx_a dx_b$, one easily obtains the following expression

$$\frac{d\hat{\sigma}^{\text{asym}}}{dp_T^2} = \hat{\sigma}_{q\bar{q}}^{(0)}(Q^2) \frac{\alpha_s}{2\pi} \frac{1}{p_T^2} \left[A^{(1)} \ln\left(\frac{Q^2}{p_T^2}\right) + B^{(1)} \right]. \quad (\text{A1})$$

When integrating over dp_T^2 , dimensional regularization will be used to regulate the $\ln(Q^2/p_T^2)/p_T^2$ and $1/p_T^2$ singularities as $p_T \rightarrow 0$ in the above expression. In $n = 4 - 2\epsilon$ dimensions, the integral of the previous equation is

$$\hat{\sigma}^{\text{asym}}(q\bar{q} \rightarrow ZZg) = \frac{(4\pi\mu^2)^\epsilon}{\Gamma(1-\epsilon)} \frac{\alpha_s}{2\pi} \hat{\sigma}_{q\bar{q}}^{(0)}(Q^2, \epsilon) \int \frac{dp_T^2}{p_T^{2+2\epsilon}} \left[A^{(1)} \ln\left(\frac{Q^2}{p_T^2}\right) + B^{(1)} \right], \quad (\text{A2})$$

where μ is a mass parameter introduced to keep the coupling constant dimensionless and $\hat{\sigma}_{q\bar{q}}^{(0)}(Q^2, \epsilon)$ denotes the lowest order cross section for $q\bar{q} \rightarrow ZZ$ in $n = 4 - 2\epsilon$ dimensions. Performing the dp_T^2 integration, we find,

$$\hat{\sigma}^{\text{asym}}(q\bar{q} \rightarrow ZZg) = \frac{1}{\Gamma(1-\epsilon)} \left(\frac{4\pi\mu^2}{Q^2} \right)^\epsilon \frac{\alpha_s}{2\pi} \hat{\sigma}_{q\bar{q}}^{(0)}(Q^2, \epsilon) \left[\frac{A^{(1)}}{\epsilon^2} - \frac{B^{(1)}}{\epsilon} \right] + \text{finite terms}. \quad (\text{A3})$$

The $1/\epsilon^2$ and $1/\epsilon$ pole terms in Eq. (A3) are the remaining pole terms after the mass factorization for the real emission subprocess $q\bar{q} \rightarrow ZZg$. Therefore, to extract the coefficients $A^{(1)}$

and $B^{(1)}$, one may start with the $\mathcal{O}(\alpha_s)$ perturbative formula for the real emission subprocess in Ref. [8]. The infrared and collinear poles can be extracted by taking the limit $p_T \rightarrow 0$. After factorizing the pure collinear $1/\epsilon$ poles into the parton distribution functions, one can compare the remaining poles with the asymptotic expression in Eq. (A3) to obtain the coefficients. Alternatively, since the remaining pole terms for the real emission subprocess $q\bar{q} \rightarrow ZZg$ will exactly cancel the soft pole terms from the one-loop virtual diagrams, one can start with the formula for the one-loop virtual correction. Here we will give the derivation according to the latter approach. The pole terms from the one-loop virtual correction to the process $q\bar{q} \rightarrow ZZ$ have been calculated[8, 9] and according to Eq. (12) of Ref. [8],

$$\hat{\sigma}^{\text{virt}}(q\bar{q} \rightarrow ZZ) = \frac{\Gamma(1-\epsilon)}{\Gamma(1-2\epsilon)} \left(\frac{4\pi\mu^2}{Q^2} \right)^\epsilon \frac{\alpha_s}{2\pi} \hat{\sigma}_{q\bar{q}}^{(0)}(Q^2, \epsilon) C_F \left[-\frac{2}{\epsilon^2} - \frac{3}{\epsilon} \right] + \text{finite terms.} \quad (\text{A4})$$

By using the fact

$$\frac{1}{\Gamma(1-\epsilon)} \approx \frac{\Gamma(1-\epsilon)}{\Gamma(1-2\epsilon)}, \quad (\text{A5})$$

to first order in ϵ and by requiring the cancelation of the pole terms between the virtual expression Eq. (A4) and real emission expression Eq. (A3), we finally obtain the result

$$A^{(1)} = 2 C_F, \quad B^{(1)} = -3 C_F, \quad (\text{A6})$$

with $C_F = 4/3$.

REFERENCES

- [1] For reviews of Higgs boson phenomenology, see, *e.g.*, J. F. Gunion, G. L. Kane, H. E. Haber, and S. Dawson, *The Higgs Hunter's Guide*, Addison Wesley, (1989); J. F. Gunion *et al.*, UC-Davis report UCD-91-0010 (1990), in *Research Directions for the Decade*, Proceedings of the Workshop, Snowmass, Colorado, (1990), (Editions Frontières, Gif-sur-Yvette, France, in press); V. Barger, in *Proceedings of the International Conference on High Energy Physics, Beyond the Standard Model II*, Norman, Oklahoma (1990), edited by K. Milton, R. Kantowski, and M. Samuel; D. Froidevaux, in *Proceedings of the LHC Workshop*, Vol. II, p. 444, Aachen, Germany (1990), edited by G. Jarlskog and D. Rein.
- [2] D. A. Dicus, C. Kao, and W. W. Repko, *Phys. Rev.* **D36**, 1570 (1987); E. W. N. Glover and J. J. van der Bij, *Nucl. Phys.* **B321**, 561 (1989).
- [3] D. A. Dicus, S. L. Wilson, and R. Vega, *Phys. Lett.* **192B**, 231 (1987); U. Baur and E. W. N. Glover, *Nucl. Phys.* **B347**, 12 (1990).
- [4] V. Barger, K. Cheung, T. Han, J. Ohnemus, and D. Zeppenfeld, *Phys. Rev.* **D44**, 1426 (1991).
- [5] R. W. Brown and K. O. Mikaelian, *Phys. Rev.* **D19**, 922 (1979); E. Eichten, I. Hinchliffe, K. Lane, and C. Quigg, *Rev. Mod. Phys.* **56**, 579 (1984); **58**, 1065(E) (1986).
- [6] U. Baur, E. W. N. Glover, and J. J. van der Bij, *Nucl. Phys.* **B318**, 106 (1989).
- [7] V. Barger, T. Han, J. Ohnemus, and D. Zeppenfeld, *Phys. Rev.* **D41**, 2782 (1990).
- [8] J. Ohnemus and J. F. Owens, *Phys. Rev.* **D43**, 3626 (1991).

- [9] B. Mele, P. Nason, and G. Ridolfi, Nucl. Phys. **B357**, 409 (1991).
- [10] R. N. Cahn *et al.*, Phys. Rev. **D35**, 1626 (1987); V. Barger, T. Han, and R. J. N. Phillips, Phys. Rev. **D37**, 2005 (1988); R. Kleiss and W. J. Stirling, Phys. Lett. **200B**, 193 (1988).
- [11] V. Barger, T. Han, and R. J. N. Phillips, Phys. Lett. **206B**, 339 (1988); U. Baur and E. W. N. Glover, Phys. Rev. **D44**, 99(1990); A. Nisati, in *Proceedings of the LHC Workshop*, Vol. II, p. 492, Aachen, Germany (1990), edited by G. Jarlskog and D. Rein.
- [12] M. S. Chanowitz and M. K. Gaillard, Nucl. Phys. **B261**, 379 (1985); M. S. Chanowitz, Annu. Rev. Nucl. Part. Sci. **38**, 323 (1988).
- [13] R. Kauffman, Phys. Rev. **D44**, 1415 (1991); UC-Davis report UCDPHYS-PUB-91-17 (1991).
- [14] Yu. L. Dokshitzer, D. I. Dyakonov, and S. I. Troyan, Phys. Lett. **78B**, 290 (1978); Phys. Rep. **58**, 269 (1980); G. Parisi and R. Petronzio, Nucl. Phys. **B154**, 427 (1979); F. Halzen, A. D. Martin, and D. M. Scott, Phys. Lett. **122B**, 160 (1982).
- [15] J. Collins and D. Soper, Nucl. Phys. **B193**, 381 (1981); **B197**, 446 (1982); **B213**, 545E (1983); J. Collins, D. Soper, and G. Sterman, Nucl. Phys. **B250**, 199 (1985).
- [16] C. Davies, B. Webber, and W. J. Stirling, Nucl. Phys. **B256**, 413 (1985).
- [17] G. Altarelli, R. K. Ellis, M. Greco, and G. Martinelli, Nucl. Phys. **B246**, 12 (1984).
- [18] P. Arnold and R. Kauffman, Nucl. Phys. **B349**, 381 (1991).
- [19] E. Berger and R. Meng, Argonne National Laboratory report ANL-HEP-PR-91-34 (1991); E. Laenen, W. L. van Neerven, and J. Smith, State University of New York at Stony Brook report ITP/SB/91/14 (1991).
- [20] We used the version PYTHIA48 and JETSET63, see, *e.g.*, H. U. Bengtsson and T. Sjos-

trand, UCLA report UCLA-87-001 (1987) (unpublished).

- [21] See Eq. (2.4) of Ref. [18]. Note that the overall minus sign in this equation was a typographical error.
- [22] W. A. Bardeen, A. J. Buras, D. W. Duke, and T. Muta, Phys. Rev. **D18**, 3998 (1978); A. J. Buras, Rev. Mod. Phys. **52**, 199 (1980).
- [23] P. N. Harriman, A. D. Martin, R. G. Roberts, and W. J. Stirling, Phys. Rev. **D42**, 798 (1990).
- [24] J. Morfin and W.-K. Tung, Fermilab report FERMILAB-PUB-90/74, to appear in Z. Phys. **C**.
- [25] V. Barger, J. L. Lopez, and W. Putikka, Int. J. Mod. Phys. **A3**, 2181 (1988).
- [26] G. 't Hooft and M. Veltman, Nucl. Phys. **B44**, 189 (1972).

FIGURES

FIG. 1. The differential distribution $d^2\sigma/dQ dp_T$ versus p_T for the LHC center of mass energy, $\sqrt{S} = 15.4$ TeV. Parts a), b), and c) are for $Q = 200, 500,$ and 800 GeV, respectively. The perturbative, asymptotic, resummed, and full matched results are shown.

FIG. 2. Same as Fig. 1 except the center of mass energy is for the SSC, $\sqrt{S} = 40$ TeV.

FIG. 3. The Z -pair transverse momentum distribution. Parts a) and b) are for the LHC and SSC center of mass energies, respectively. The resummed, perturbative, and full matched results are shown. Also shown is the result from the Monte Carlo program PYTHIA. Kinematical cuts of Eq. (33) have been imposed here.

FIG. 4. The differential distribution $d^2\sigma/dQ dp_T$ versus p_T at $Q = 200$ GeV for the SSC center of mass energy. Results for three sets of the non-perturbative parameters g_1 and g_2 , corresponding to Eqs. (29), (34), and (35), are shown.

FIG. 5. The differential distribution $d^2\sigma/dQ dp_T$ versus p_T at $Q = 200$ and 800 GeV for the SSC center of mass energy. Results from the HMRS Set B and the MT Set B1 parton distribution functions are shown.

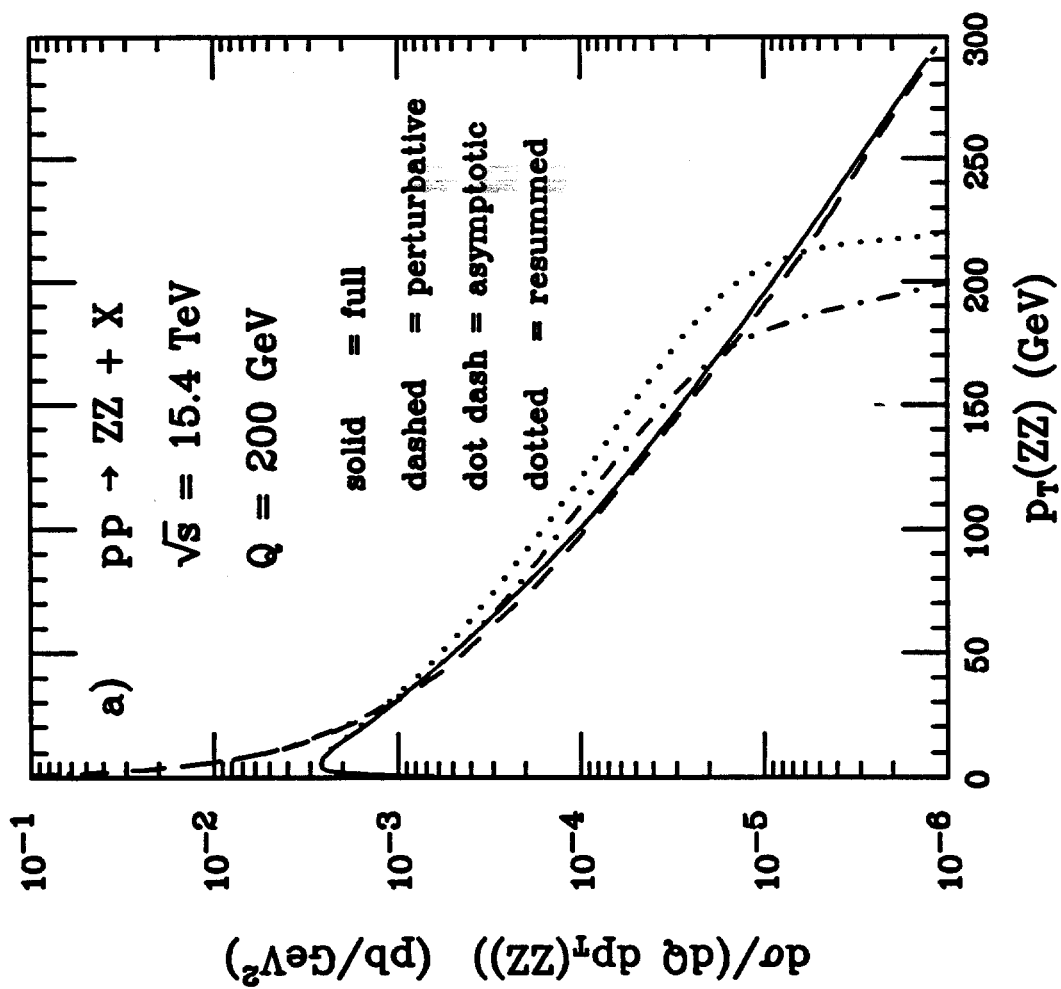


Figure 1

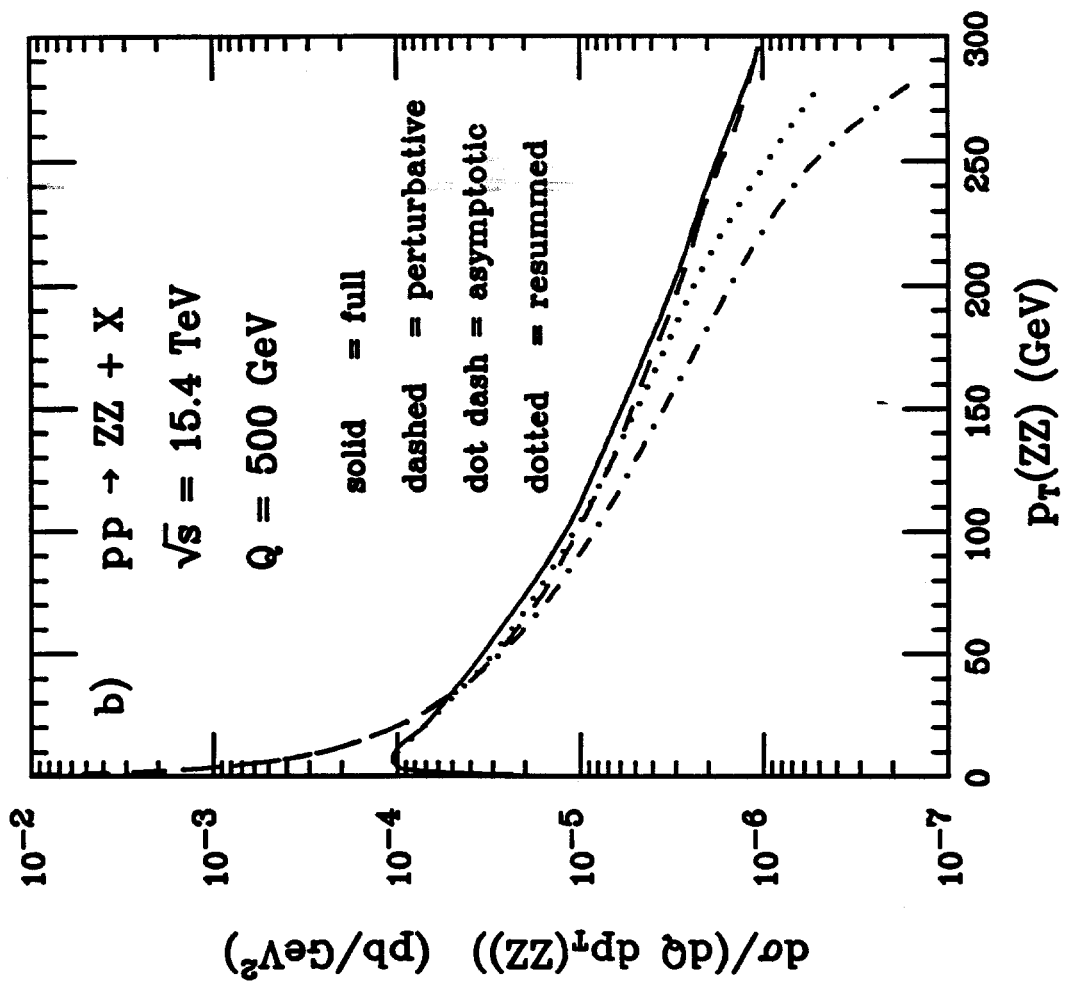


Figure 1

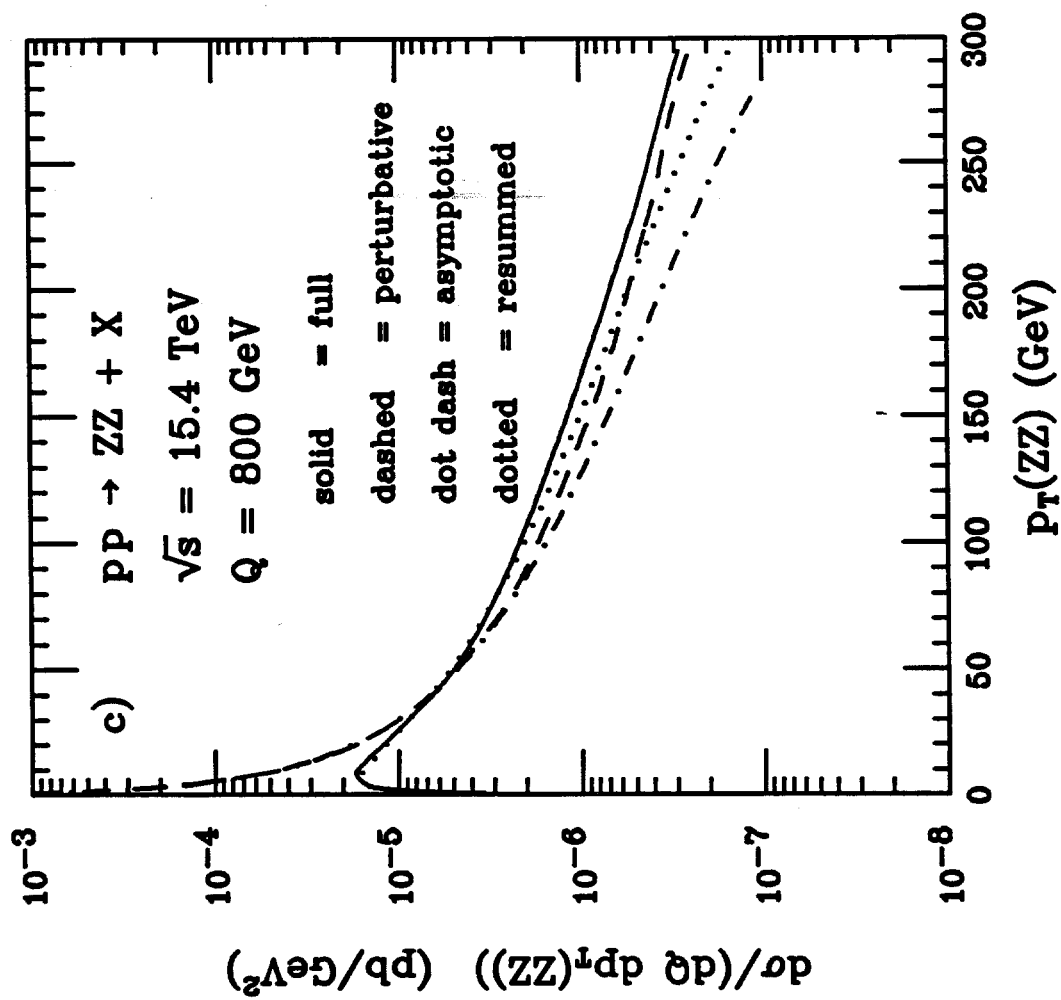


Figure 1

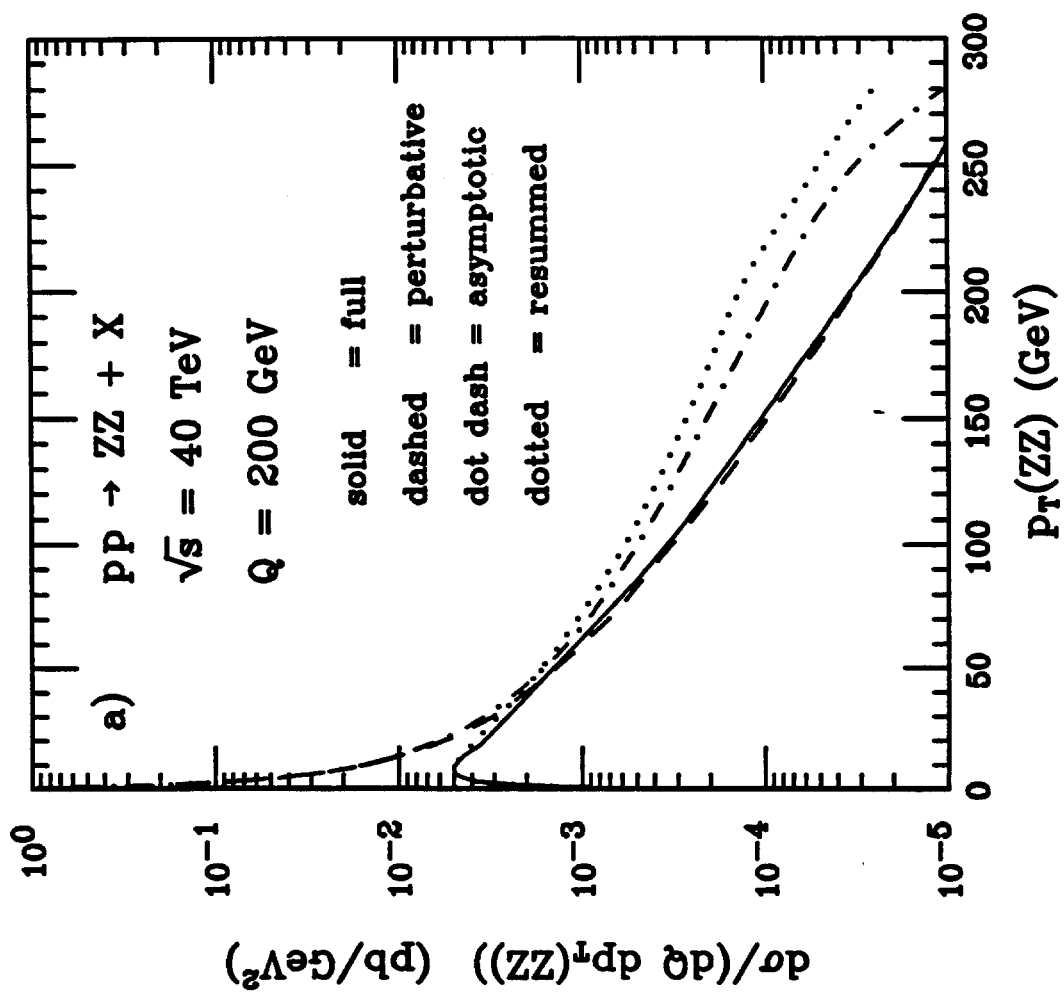


Figure 2

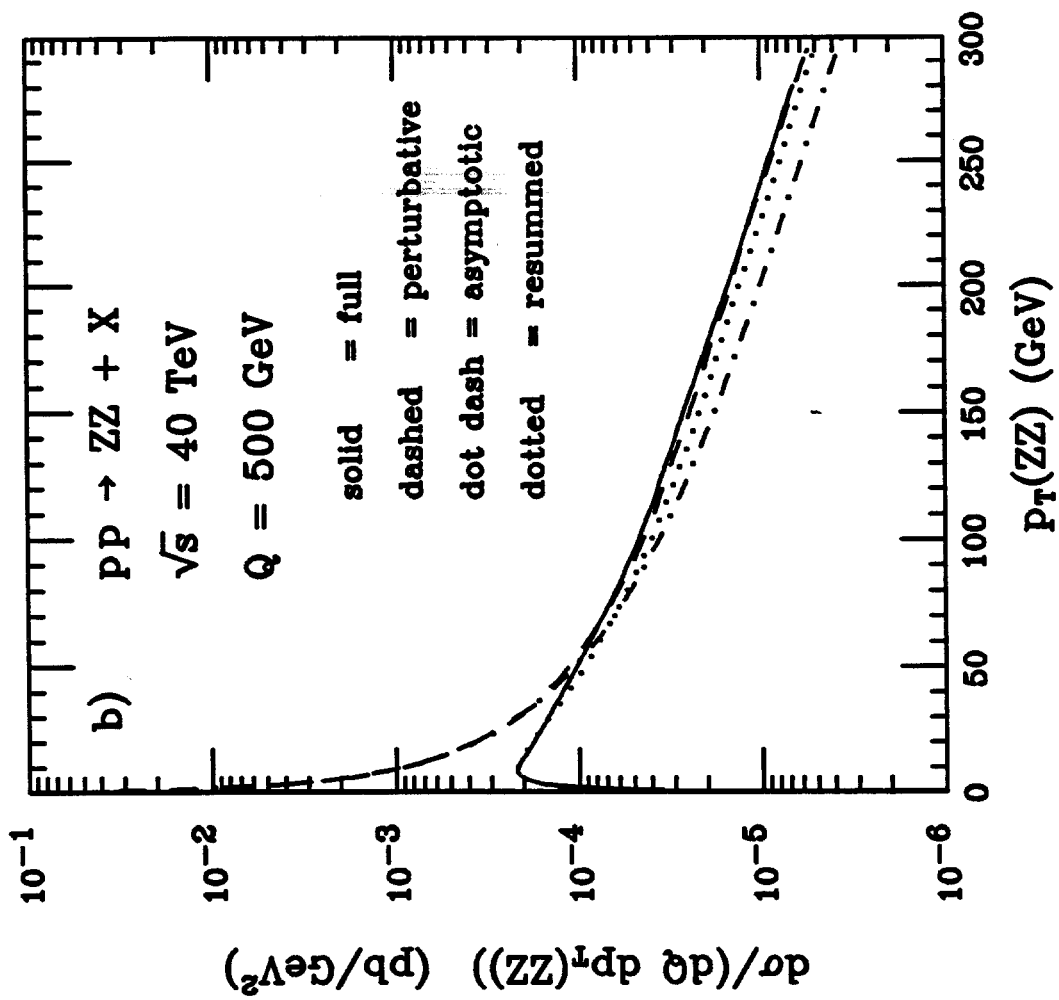


Figure 2

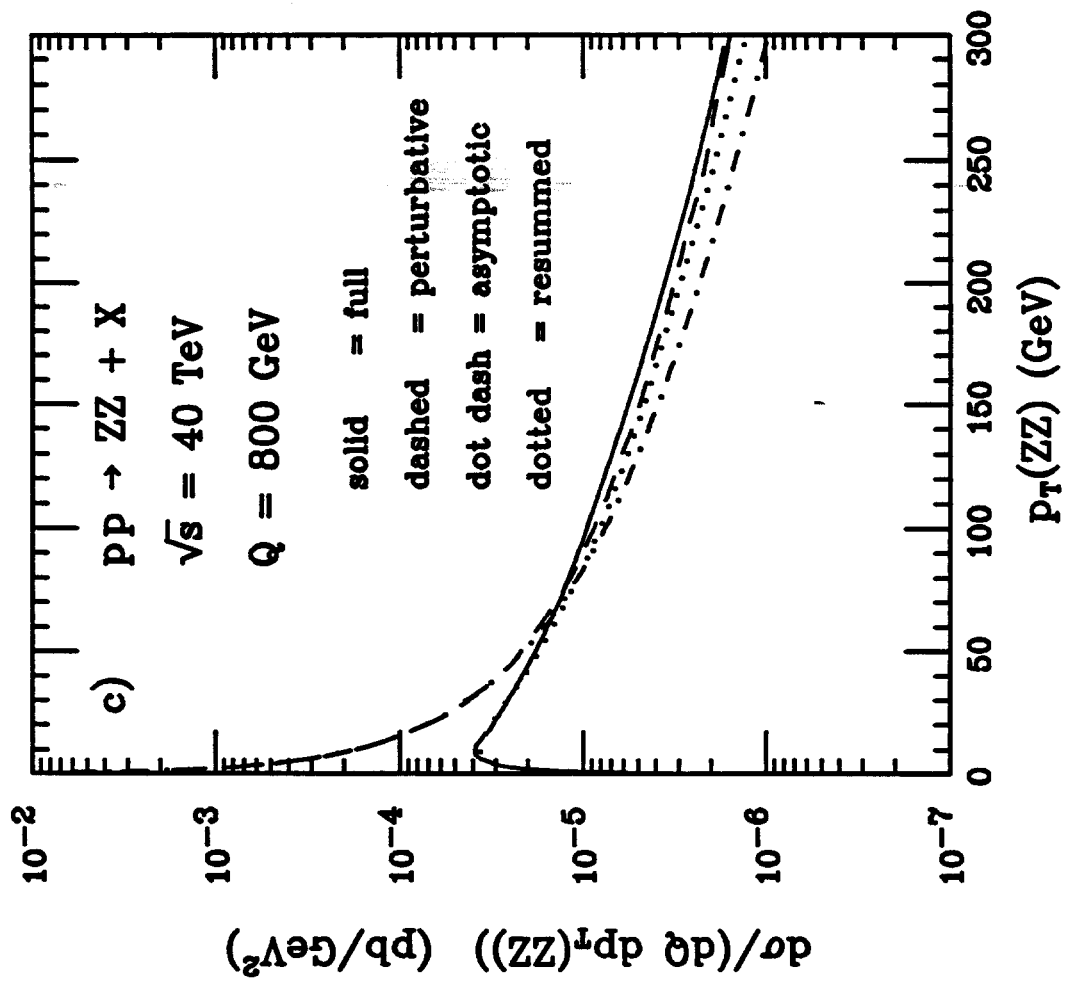


Figure 2

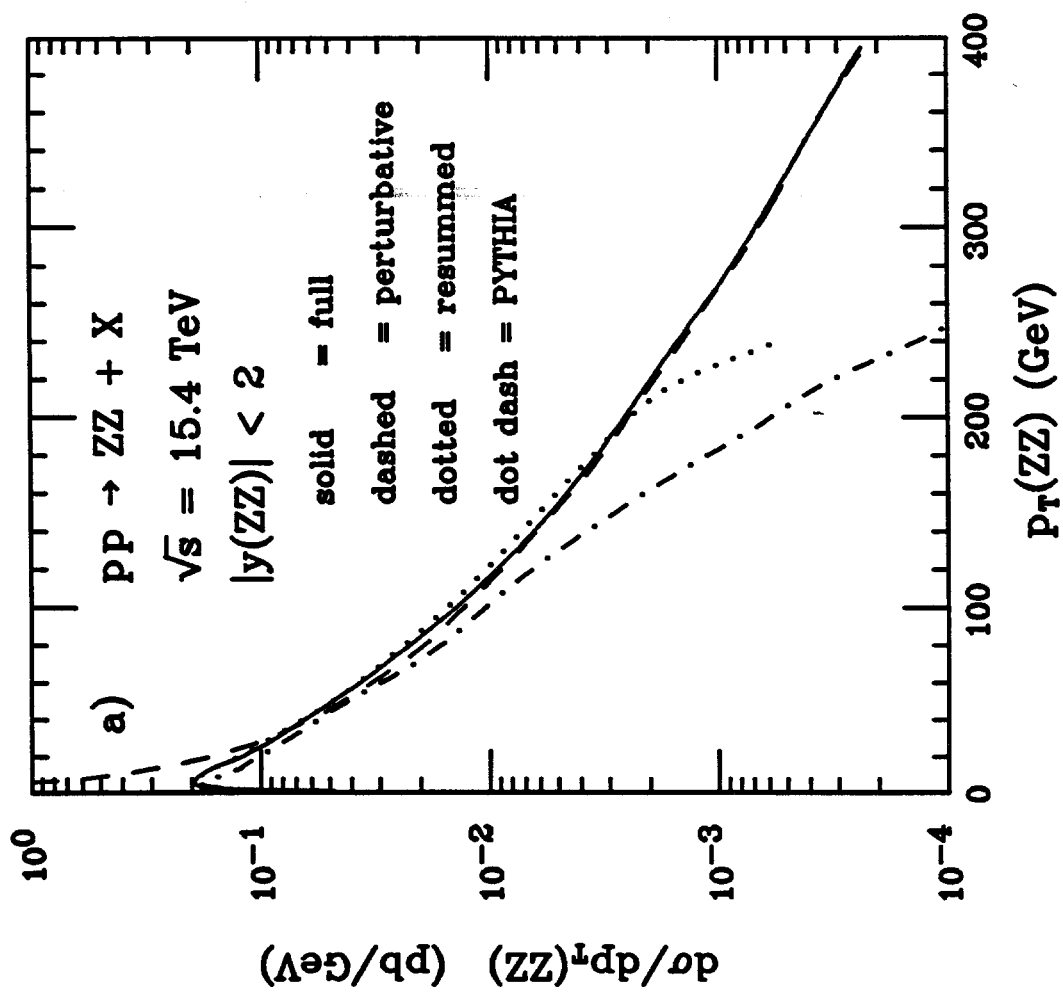


Figure 3

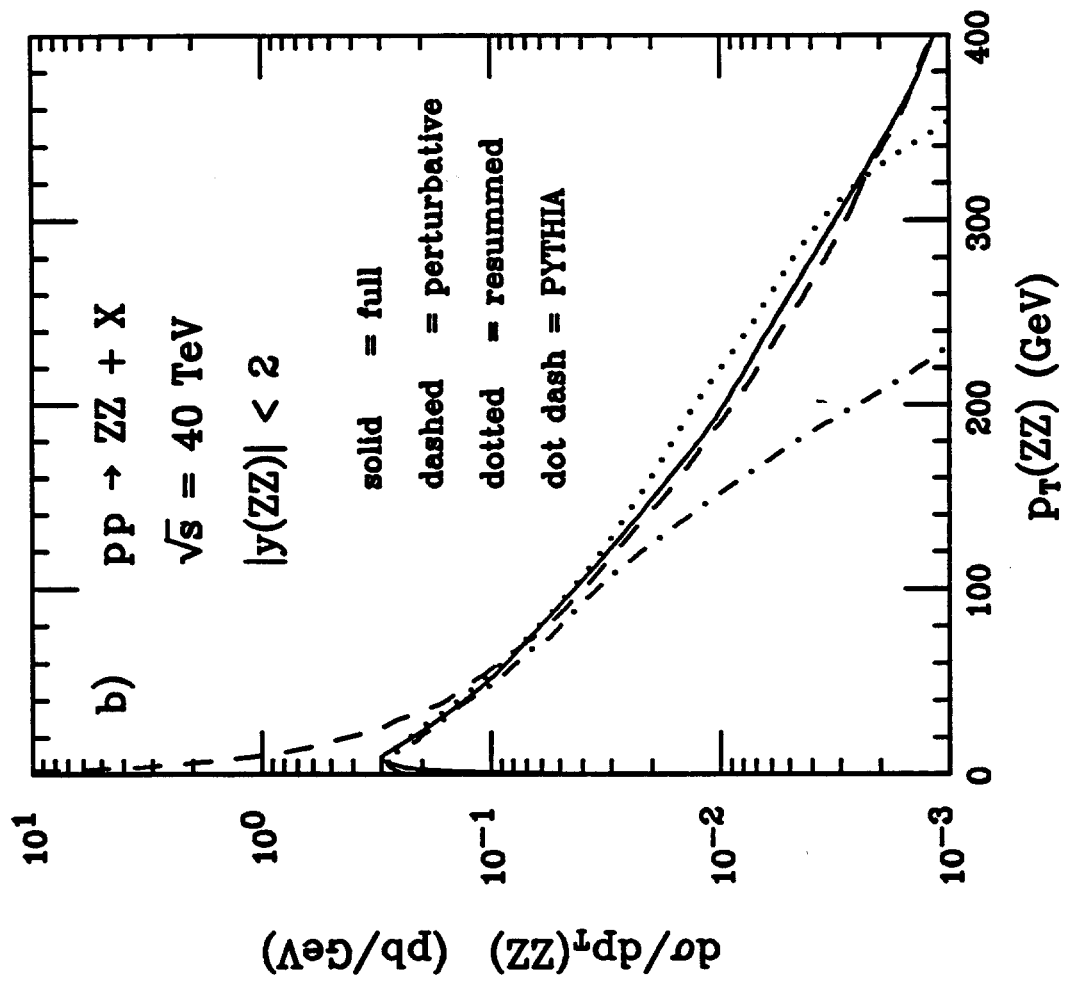


Figure 3

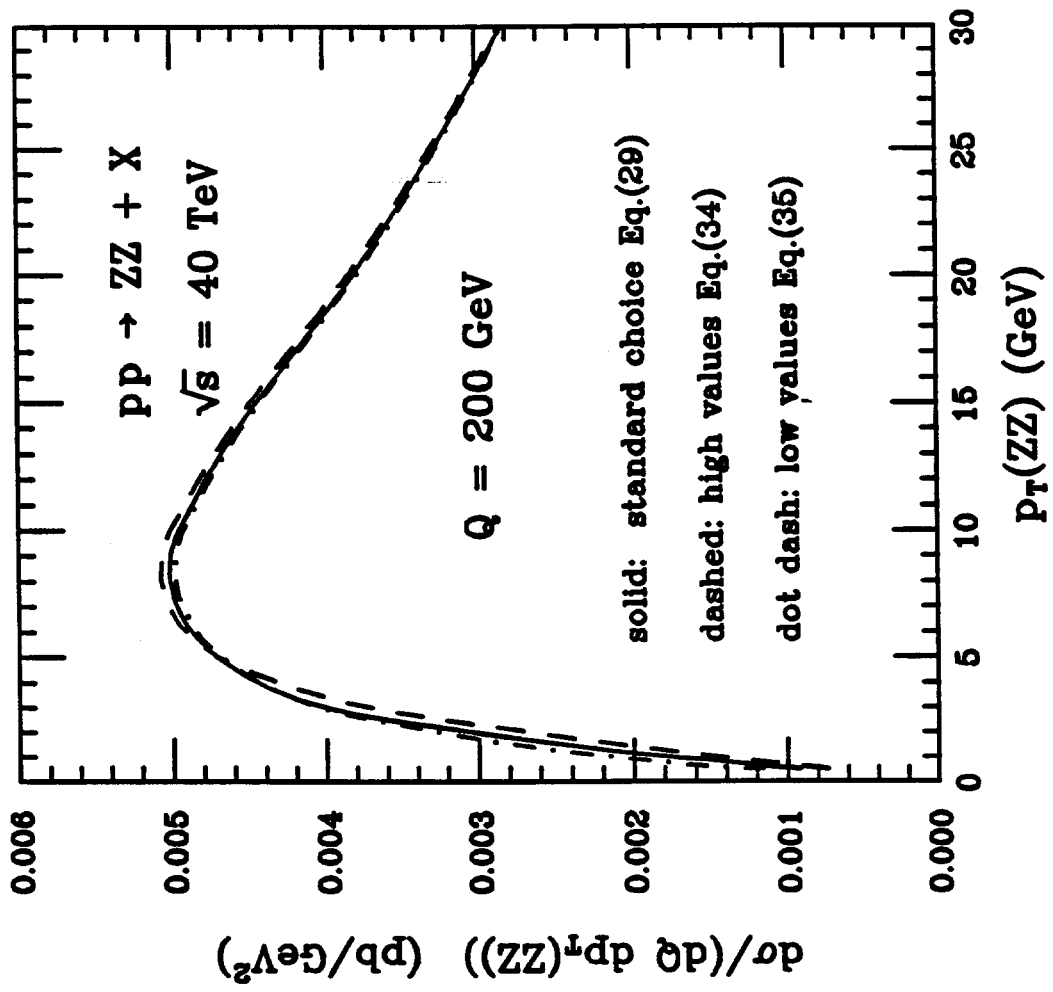


Figure 4

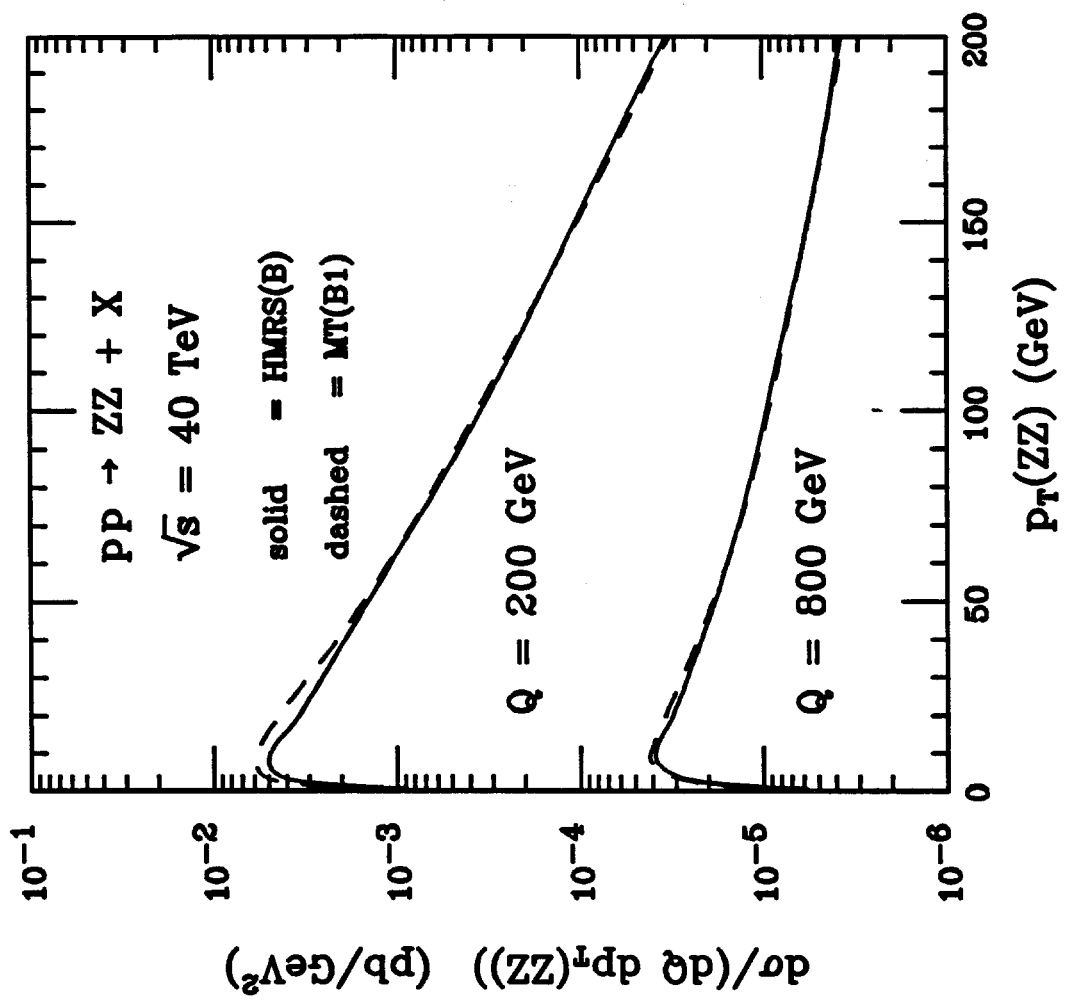


Figure 5